Published March 30, 2015



# A single glycan on IgE is indispensable for initiation of anaphylaxis

Kai-Ting C. Shade,[1] Barbara Platzer,[2,3] Nathaniel Washburn,[4] Vinidhra Mani,[1] Yannic C. Bartsch,[1] Michelle Conroy,[1] Jose D. Pagan,[1] Carlos Bosques,[4] Thorsten R. Mempel,[1] Edda Fiebiger,[2,3] and Robert M. Anthony[1]

[1]Center for Immunology and Inflammatory Diseases, Division of Rheumatology, Allergy, and Immunology, Massachusetts General Hospital, Harvard Medical School, Charlestown, MA 02129
[2]Division of Gastroenterology, Hepatology, and Nutrition, Boston Children's Hospital and [3]Department of Pediatrics, Harvard Medical School, Boston, MA 02115
[4]Momenta Pharmaceuticals, Cambridge, MA 02142

**Immunoglobulin ε (IgE) antibodies are the primary mediators of allergic diseases, which affect more than 1 in 10 individuals worldwide. IgE specific for innocuous environmental antigens, or allergens, binds and sensitizes tissue-resident mast cells expressing the high-affinity IgE receptor, FcεRI. Subsequent allergen exposure cross-links mast cell–bound IgE, resulting in the release of inflammatory mediators and initiation of the allergic cascade. It is well established that precise glycosylation patterns exert profound effects on the biological activity of IgG. However, the contribution of glycosylation to IgE biology is less clear. Here, we demonstrate an absolute requirement for IgE glycosylation in allergic reactions. The obligatory glycan was mapped to a single N-linked oligomannose structure in the constant domain 3 (Cε3) of IgE, at asparagine-394 (N394) in human IgE and N384 in mouse. Genetic disruption of the site or enzymatic removal of the oligomannose glycan altered IgE secondary structure and abrogated IgE binding to FcεRI, rendering IgE incapable of eliciting mast cell degranulation, thereby preventing anaphylaxis. These results underscore an unappreciated and essential requirement of glycosylation in IgE biology.**

CORRESPONDENCE
Robert M. Anthony:
robert.anthony@mgh.harvard.edu

Abbreviations used: CD, circular dichroism; DNP, dinitrophenol; EndoF1, endoglycosidase F1; mBMMC, mouse BM-derived mast cell; MFI, mean fluorescent intensity; PCA, passive cutaneous anaphylaxis; PNG, peptide-*N*-glycosidase F; polymIgE, polyclonal mouse IgE; TNP, trinitrophenol.

Immunoglobulin ε (IgE) is important for resistance to parasitic infections (Dombrowicz et al., 1996; Gould et al., 2003; Matsumoto et al., 2013) and protection against venom toxins (Arnold et al., 2007; Marichal et al., 2013; Palm et al., 2013). Yet IgE is also responsible for triggering allergic reactions, one of the most common chronic conditions worldwide (Dorrington and Bennich, 1978; Arnold et al., 2007; Pawankar et al., 2013; Plomp et al., 2014). These diseases include asthma and atopic dermatitis, as well as allergies to food, dust mites, insect venom, pollen, and pet dander. Allergic reactions manifest as localized wheel and flare irritations, can have respiratory symptoms, including sneezing, rhinitis, and asthma, and in extreme cases can be life threatening in the form of anaphylaxis. Although IgE is the least abundant Ig in circulation, with a short serum half-life, it persists for weeks bound to the surface of mast cells by the high-affinity IgE receptor, FcεRI, in tissues (Gould et al., 2003). Cross-linking of mast cell–bound IgE by allergens activates the cells and results in release of mediators that induce vasodilation, vascular permeability, and smooth muscle contractility (Gould et al., 2003; Galli and Tsai, 2012).

IgE is the most heavily glycosylated monomeric Ig in mammals, with seven N-linked glycosylation consensus sequences (N-X-S/T) distributed across each heavy chain of human IgE (Arnold et al., 2007). The importance of glycosylation in Ig biology is increasingly appreciated. For example, the single glycan on IgG at N297 is essential for structural integrity of the constant fragment (Fc), and without it IgG cannot engage Fcγ receptors (Feige et al., 2009). However, the precise role of glycosylation to IgE biology is less clear. Some studies concluded glycosylation of IgE is essential for

© 2015 Shade et al. This article is distributed under the terms of an Attribution–Noncommercial–Share Alike–No Mirror Sites license for the first six months after the publication date (see http://www.rupress.org/terms). After six months it is available under a Creative Commons License (Attribution–Noncommercial–Share Alike 3.0 Unported license, as described at http://creativecommons.org/licenses/by-nc-sa/3.0/).

The Rockefeller University Press $30.00
J. Exp. Med. 2015 Vol. 212 No. 4 457–467
www.jem.org/cgi/doi/10.1084/jem.20142182

Supplemental Material can be found at:
http://jem.rupress.org/content/suppl/2015/03/24/jem.20142182.DC1.html



The Journal of Experimental Medicine

Downloaded from jem.rupress.org on April 10, 2015

Published March 30, 2015



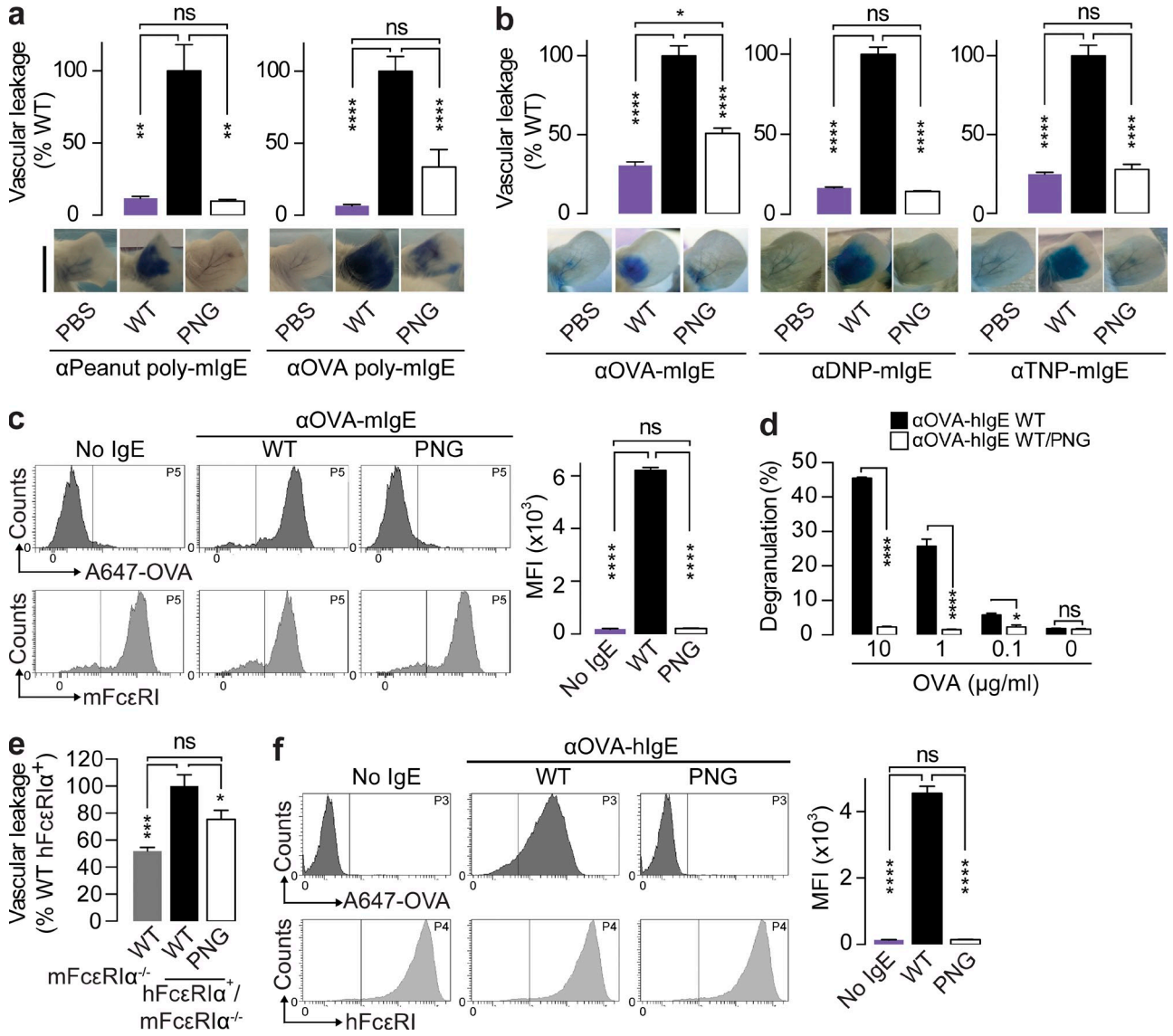


**Figure 1. N-linked glycosylation is essential for IgE-mediated allergic inflammation.** (a and b) Quantified vascular leakage and representative ear images after PCA with PBS, WT, or PNG–poly-mIgE specific for OVA or peanut extracts ($n$ = 4 ears; 2 independent experiments; a) or monoclonal mIgE specific for OVA, DNP, or TNP ($n$ = 8; 2, 3, and 3 independent experiments for OVA, DNP, and TNP; b). Bar, 1 cm. (c) Histograms and mean fluorescent intensity (MFI) of WT or PNG-αOVA-mIgE binding to mBMMCs determined by A647-OVA and mFcεRI ($n$ = 3; 2 independent experiments). (d) β-Hexosaminidase activity after OVA stimulation of LAD2 cell sensitized with WT or PNG-treated αOVA-hIgE ($n$ = 3; 5 independent experiments). (e) Quantified OVA-induced PCA in mFcεRI$^{-/-}$ or hFcεRI$^{+}$mFcεRI$^{-/-}$ mice sensitized by WT or PNG-αOVA-hIgE ($n$ = 4; 2 independent experiments). (f) FACS of WT or PNG-αOVA-hIgE to hFcεRI$^{+}$-HeLa cells assessed by A647-OVA and α-hFcεRI-PE ($n$ = 2; 2 independent experiments). Means and SEM are plotted; ****, P < 0.0001; ***, P < 0.001; **, P < 0.01; *, P < 0.05; ns, not significant.

FcεRI binding and effector functions (Nettleton and Kochan, 1995; Sayers et al., 1998; Björklund et al., 1999; 2000; Hunt et al., 2005). However, these findings have been contradicted (Basu et al., 1993; Young et al., 1995), supported by studies using a functional aglycosylated IgE derived from *Escherichia coli* (Helm et al., 1988; Henry et al., 2000). Therefore, we sought to determine whether glycosylation was required for the in vivo activity of IgE.

We conducted a systematic analysis of all glycosylation sites on mouse and human IgE, which revealed a single glycan in the IgE Cε3 domain to be essential for triggering anaphylaxis. This site was occupied almost exclusively by oligomannose glycans, whereas complex antennary glycans were found at the other sites throughout mouse and human IgE. Selective enzymatic removal of the oligomannose glycan altered secondary structure of IgE, prevented binding to FcεRI on mast cells, and importantly, attenuated anaphylaxis in vivo. Together, the findings herein identify the IgE oligomannose glycan essential for in vivo activity and structural integrity of this Ig class.

Downloaded from jem.rupress.org on April 10, 2015

Published March 30, 2015



## RESULTS AND DISCUSSION

### Enzymatic deglycosylation attenuates IgE

To generate polyclonal mouse IgE (poly-mIgE), we immunized mice with OVA or extract from the common food allergen peanuts in alum. The mice were bled and IgG depleted from the serum. All N-linked glycans were removed from the poly-mIgE by treatment with the endoglycosidase peptide-*N*-glycosidase F (PNG). This treatment did not reduce recognition of peanuts or OVA by poly-mIgE, as determined by ELISA (unpublished data). Next, we injected poly-mIgE intradermally into the ears of mice in a model of passive cutaneous anaphylaxis (PCA), highly dependent on the interactions between IgE, Fc$\varepsilon$RI$^+$ mast cells, and allergens (Dombrowicz et al., 1993), and the next day intravenously challenged with appropriate allergens and Evan's blue dye. Poly-mIgE elicited robust anaphylaxis to peanuts or OVA, as measured by vascular leakage of the blue dye. However, after treatment with PNG, poly-mIgE induced significantly decreased anaphylaxis to either allergen (Fig. 1 a). Next, we treated three monoclonal mIgEs specific for model allergens OVA, dinitrophenol (DNP), or trinitrophenol (TNP) with PNG. Enzymatic deglycosylation and antigen binding were verified by lectin blotting and ELISA assays, respectively (unpublished data). Although mIgE specific for OVA, DNP, or TNP triggered strong allergen-specific anaphylactic responses in vivo, PNG treatment significantly attenuated vascular leakage (Fig. 1 b).

Allergic reactions are highly dependent on IgE and Fc$\varepsilon$RI interactions (Dombrowicz et al., 1993; Gould et al., 2003). To determine the contribution of glycosylation to interactions with mouse Fc$\varepsilon$RI (mFc$\varepsilon$RI), mouse BM-derived mast cells (mBMMCs) were sensitized in vitro with native or deglycosylated $\alpha$OVA-mIgE overnight. When ligand–receptor interactions were analyzed by flow cytometry using Alexa Fluor 647–OVA (A647-OVA), we found that although $\alpha$OVA-mIgE bound to the mast cells, PNG-$\alpha$OVA-mIgE did not (Fig. 1 c). Indeed, WT-mIgE specific for OVA, DNP, or TNP, but not PNG-mIgE, was able to activate mBMMCs upon antigen stimulation (not depicted). Together, these results demonstrate that mIgE glycosylation is necessary for mast cell binding in vitro and eliciting anaphylaxis to multiple antigens in vivo.

We next generated and enzymatically deglycosylated OVA-specific human IgE ($\alpha$OVA-hIgE, PNG-$\alpha$OVA-hIgE) and sensitized human LAD2 mast cells in vitro with these preparations. OVA stimulation resulted in dose-dependent degranulation of $\alpha$OVA-hIgE–sensitized mast cells, as assessed by $\beta$-hexosaminidase release. Consistent with our results, PNG-$\alpha$OVA-hIgE was incapable of instigating degranulation upon OVA stimulation (Fig. 1 d). In parallel, we administered $\alpha$OVA-hIgE or PNG-$\alpha$OVA-hIgE intradermally to transgenic mice expressing human Fc$\varepsilon$RI while lacking mFc$\varepsilon$RI (hFc$\varepsilon$RI$^+$/mFc$\varepsilon$RI$^{-/-}$; Dombrowicz et al., 1996). These transgenic mice have a broad cellular distribution of hFc$\varepsilon$RI expression, whereas mFc$\varepsilon$RI is restricted to mast cells and basophils in the WT mice. hIgE is unable to elicit PCA in mFc$\varepsilon$RI$^{-/-}$ mice, which served as an injection control group. $\alpha$OVA-hIgE triggered robust vascular leakage in the ears of hFc$\varepsilon$RI$^+$/mFc$\varepsilon$RI$^{-/-}$ mice upon OVA challenge (Fig. 1 e). The response was significantly diminished in PNG-$\alpha$OVA-hIgE–treated ears (Fig. 1 e), confirming N-linked glycosylation is also essential for the in vivo activity of human IgE.

To determine whether hIgE glycosylation was important for hFc$\varepsilon$RI binding, HeLa cells engineered to express hFc$\varepsilon$RI (hFc$\varepsilon$RI$^+$-HeLa) were sensitized with $\alpha$OVA-hIgE, incubated with A647-OVA, and analyzed by flow cytometry. Although $\alpha$OVA-hIgE bound to hFc$\varepsilon$RI$^+$-HeLa cells was detected by A647-OVA, PNG-$\alpha$OVA-hIgE did not (Fig. 1 f), despite recognizing OVA by ELISA (not depicted). Together, these results indicate that IgE glycosylation is essential for the initiation of anaphylaxis and Fc$\varepsilon$RI interactions.

### Mapping glycosylation requirements of IgE

We generated a panel of $\alpha$OVA-mIgE mutants selectively lacking all glycosylation sites on each constant domain (C$\varepsilon$1–4) by mutating asparagine (N) to glutamine (Q). After confirming that all domain-specific mutants recognized OVA similarly (not depicted), these antibodies were tested in vivo by PCA. Although C$\varepsilon$2- or C$\varepsilon$4-$\alpha$OVA-mIgE domain mutants promoted robust vascular leakage after OVA challenge similar to WT (Fig. 2 a), C$\varepsilon$1-$\alpha$OVA-mIgE glycosylation mutants exhibited slightly enhanced vascular leakage. In contrast, anaphylaxis elicited by the C$\varepsilon$3-$\alpha$OVA-mIgE mutant was significantly attenuated. WT-, C$\varepsilon$1-, C$\varepsilon$2-, and C$\varepsilon$4-$\alpha$OVA-mIgE activated mBMMCs upon OVA stimulation, but C$\varepsilon$3-$\alpha$OVA-mIgE did not (not depicted). $\alpha$OVA-hIgE domain–specific glycosylation mutants were also generated and tested for mast cell degranulating activity (Fig. 2 b). WT- and C$\varepsilon$2-$\alpha$OVA-hIgE domain mutants triggered robust degranulation upon OVA stimulation. Although degranulation was slightly reduced in mast cells sensitized with C$\varepsilon$1-$\alpha$OVA-hIgE, mutation of C$\varepsilon$3 glycosylation sites completely abolished OVA-specific degranulation. Importantly, C$\varepsilon$1-$\alpha$OVA-hIgE mutants bound to Fc$\varepsilon$RI$^+$-HeLa cells, as determined by A647-OVA flow cytometry, but C$\varepsilon$3-$\alpha$OVA-hIgE did not (Fig. 2 c). Together, these results indicate that C$\varepsilon$1 glycosylation plays a minor role in modulating IgE functions, perhaps by controlling Fab arm flexibility (Arnold et al., 2007), but is not involved in Fc$\varepsilon$RI binding. More importantly, C$\varepsilon$3 glycosylation is required for both mouse and human IgE to bind Fc$\varepsilon$RI and initiate anaphylaxis.

### An obligate IgE C$\varepsilon$3 glycan

To dissect the importance of the two N-linked glycosylation sites in C$\varepsilon$3 of mIgE, individual glycosylation site mutants were generated by conversion of N361 or N384 to Q. Both WT- and N361Q-$\alpha$OVA-mIgE elicited a robust anaphylactic response in vivo, but N384Q-$\alpha$OVA-mIgE did not (Fig. 3 a). Moreover, a reciprocal mutant, in which all N-linked glycosylation sites were disrupted except N384 (N384only-$\alpha$OVA-mIgE), promoted a strong PCA upon OVA administration (Fig. 3 a). To confirm the importance of N384 glycosylation for mIgE function, the glycosylation consensus sequence was

Downloaded from jem.rupress.org on April 10, 2015

Published March 30, 2015



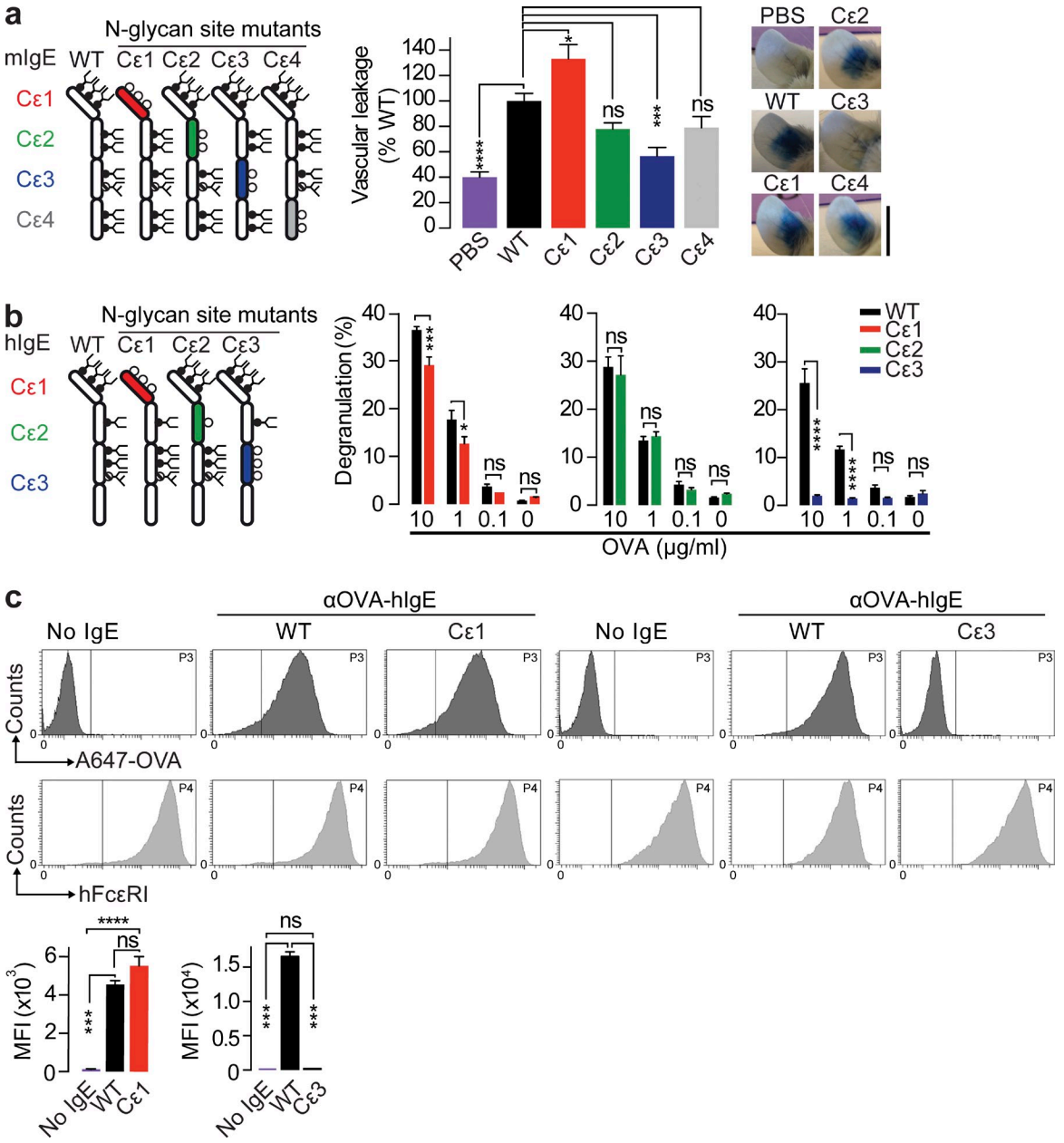


**Figure 2. Glycosylation of IgE Cε3 is required for anaphylaxis and FcεRI binding.** (a) Quantified OVA-specific PCA by PBS, WT, or αOVA-mIgE domain mutants ($n$ = 8; 3 independent experiments). Bar, 1 cm. (b) β-Hexosaminidase activity after OVA-induced degranulation in LAD2 cells sensitized with WT or αOVA-hIgE glycomutants ($n$ = 3; 3 independent experiments). (c) WT-αOVA-hIgE or Cε1- and Cε3-αOVA-hIgE glycosylation mutant binding to hFcεRI⁺-HeLa cells assessed by A647-OVA and α-hFcεRI-PE FACS ($n$ = 2; 2 independent experiments). Mean and SEM are plotted; ****, $P < 0.0001$; ***, $P < 0.001$; *, $P < 0.05$; ns, not significant.

disrupted by mutation of the third-position amino acid (T386A). Indeed, T386A-αOVA-mIgE could not initiate anaphylaxis (Fig. 3 a). Neither N384Q- nor T386A-αOVA-mIgE was able to activate mBMMCs in vitro (not depicted). Collectively, our data reveal glycosylation specifically at N384 in the Cε3 domain of mIgE is key for initiation of anaphylaxis.

We hypothesized that N384 was required for mIgE binding to FcεRI on mast cells. To test this in vivo, equal amounts of A488- and A568-labeled WT-αOVA-mIgE (A488-WT/A568-WT) or A488-WT-αOVA-mIgE and A568-N384Q-αOVA-mIgE (A488-WT/A568-N384Q) were injected intradermally into mouse ears and assessed by flow cytometry the next day. Dermal mast cells (CD45⁺ c-Kit⁺ CD11b⁻) from WT mice bound WT-αOVA-mIgE regardless of fluorophore conjugate but preferentially bound WT- over N384Q-αOVA-mIgE when both were administered (Fig. 3 b and Fig. S1). Dermal mast cells from mFcεRI$^{-/-}$ mice showed minimal binding of WT-αOVA-mIgE, confirming the requirement

Downloaded from jem.rupress.org on April 10, 2015

Published March 30, 2015



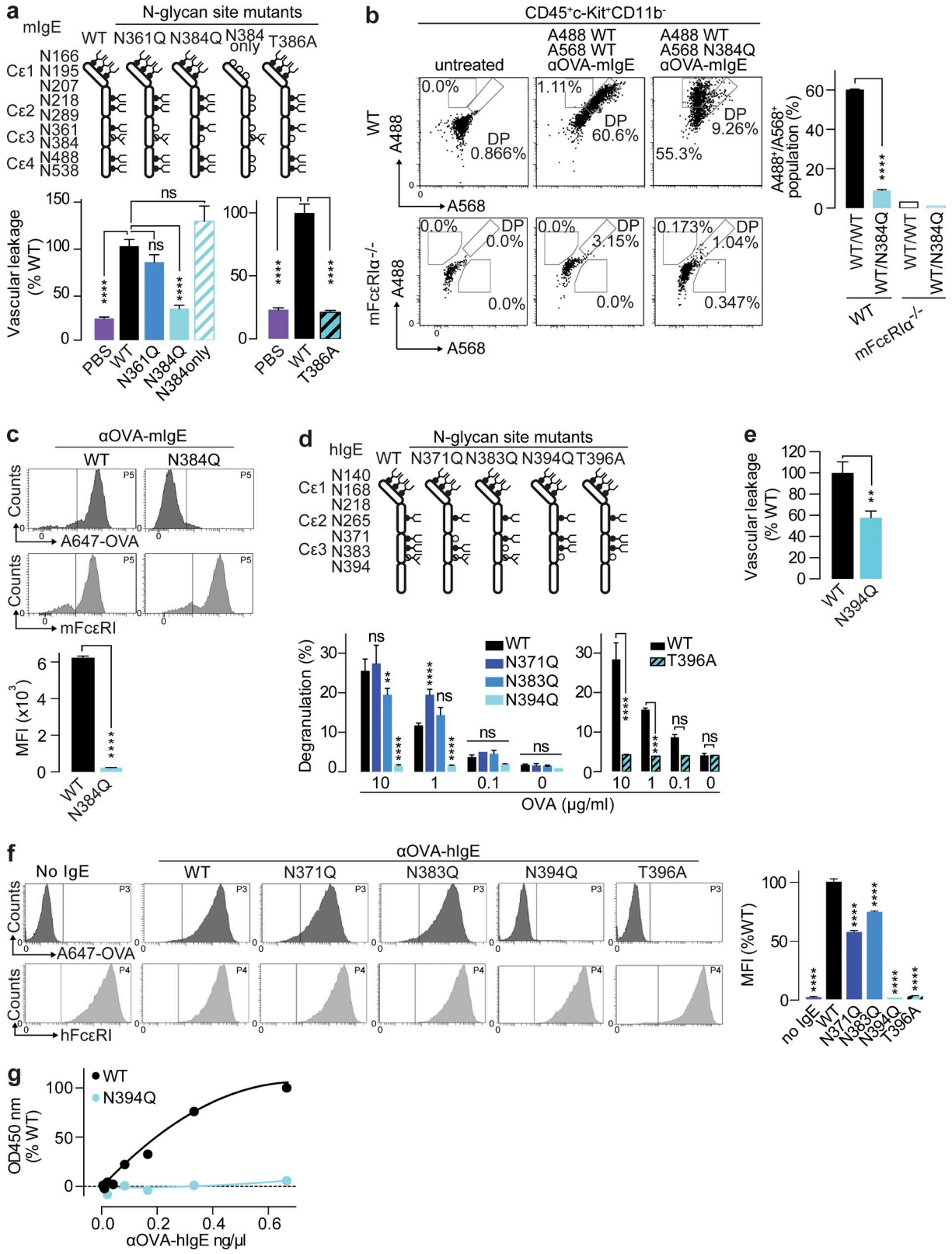


**Figure 3. A single N-linked glycosylation site is indispensable for anaphylaxis and hFcεRI binding.** (a) Quantified OVA-induced PCA with PBS, WT, or αOVA-mIgE Cε3 domain glycomutants ($n$ = 8; 3 independent experiments). (b) Scatter plots of CD45$^+$c-Kit$^+$CD11b$^-$ mast cells recovered from WT or mFcεRI$^{-/-}$ ears injected with A488-WT and A568-WT αOVA-mIgE or A488-WT and A568-N384Q αOVA-mIgE the previous day. Percentage of A488 and A568 double-positive mast cells are shown ($n$ = 2; 2 independent experiments). (c) Histograms and MFI of WT or N384Q αOVA-mIgE binding to

Downloaded from jem.rupress.org on April 10, 2015

Published March 30, 2015



of FcεRI engagement in vivo (Fig. 3 b and Fig. S1). Furthermore, N384Q-αOVA-mIgE was not bound by mast cells when injected alone, indicating the mutation and not competition with WT-αOVA-mIgE prevented mast cell engagement (not depicted). In parallel, we primed mBMMCs with WT- or N384Q-αOVA-mIgE and detected A647-OVA bound to WT- but not N384Q-αOVA-mIgE–sensitized cells (Fig. 3 c). These results demonstrate that the N384 glycan is crucial for stable mIgE interactions with mFcεRI on mast cells in vitro and in vivo.

Three Cε3 N-linked glycosylation sites are occupied in αOVA-hIgE. To determine the contribution of these sites to the initiation of anaphylaxis, individual site mutants were generated and examined for degranulation activity. N371Q- or N383Q-αOVA-hIgE exhibited slightly altered ability to activate mast cells upon OVA stimulation compared with WT. Conversely, mutation of either the first position (N394Q-αOVA-hIgE) or third position (T396A-αOVA-hIgE) of the N394 glycosylation site ablated OVA-mediated degranulation (Fig. 3 d). Furthermore, N394Q-αOVA-hIgE was unable to elicit vascular leakage by PCA in hFcεRI$^{+}$/mFcεRI$^{-/-}$ mice (Fig. 3 e). We next examined the role of N394 glycan in hFcεRI binding. Flow cytometry of hFcεRI$^{+}$-HeLa cells primed with WT-, N371Q-, N383Q-, N394Q-, or T396A-αOVA-hIgE and treated with A647-OVA revealed that WT-, N371Q-, and N383Q- but not N394Q- or T396A-αOVA-hIgE bound hFcεRI (Fig. 3 f). Furthermore, although WT-αOVA-hIgE bound and saturated immobilized hFcεRI in vitro, N394Q-αOVA-hIgE did not (Fig. 3 g). These results identify the glycans at N394 and N384 of hIgE and mIgE, respectively, as essential for interacting with FcεRI and mast cells and initiating allergen-specific inflammation.

### The IgE oligomannose is essential for in vivo activity

We analyzed site-specific glycosylation throughout the four constant domains (Cε1–4) of recombinant mouse and human αOVA-IgE by glycopeptide mass spectroscopy (Plomp et al., 2014). Eight of nine N-linked glycosylation consensus sequences in αOVA-mIgE were primarily occupied by highly processed complex biantennary glycans (Fig. 4 a and Table S1). Similarly, all but one site on αOVA-hIgE contained predominantly complex antennary structures (Fig. 4 b and Table S2). Interestingly, the glycosylation sites identified as essential for initiating anaphylaxis, N384 of mIgE and N394 of hIgE, were occupied by oligomannose glycans, consistent with previous analyses of hIgE glycosylation (Dorrington and Bennich, 1978; Arnold et al., 2007; Plomp et al., 2014).

Endoglycosidase F1 (EndoF1) selectively cleaves N-linked oligomannose and afucosylated hybrid glycans, leaving complex glycans unaffected, unlike PNG which removes all N-linked glycans. Thus, we treated mIgE specific for OVA, DNP, or TNP with EndoF1 and tested these preparations in vivo by PCA. Selective enzymatic removal of oligomannose glycans significantly attenuated vascular leakage compared with WT-mIgE (Fig. 4 c). Furthermore, EndoF1-αOVA-mIgE did not bind to mFcεRI or mast cells in vitro or in vivo, respectively (Fig. 4, d and e; and Fig. S1), nor was it able to activate mBMMCs in vitro (not depicted). These results demonstrate that the oligomannose glycan on mIgE is required for initiating anaphylaxis, interacting with mast cells, and binding mFcεRI.

Next, we treated αOVA-hIgE, biotinylated hIgE, or hIgE recovered from human allergic serum with EndoF1 and sensitized mast cells with these preparations. This treatment abolished mast cell activation after cross-linking by OVA, streptavidin, or anti–human light chain, respectively (Fig. 4 f). EndoF1 treatment also ablated hIgE binding to hFcεRI in flow cytometry and saturation binding experiments (Fig. 4, g and h). Importantly, EndoF1 treatment did not induce IgE aggregation, as assessed by size exclusion chromatography, in contrast to a previous study reporting dimerization after PNG treatment (Fig. 4 i; Basu et al., 1993).

A previous study has shown that removal of the single N-linked glycan on IgG Fc results in a conformation change that prevents FcγR binding (Feige et al., 2009). Thus, the contribution of the oligomannose glycan to hIgE secondary structure was examined by circular dichroism (CD; Sondermann et al., 2013). Although the UV CD spectra of WT– and EndoF1–buffer control hIgE overlapped, a shift was observed after EndoF1 treatment (Fig. 4 j). This likely reflects small changes in the overall secondary structure of hIgE upon oligomannose removal, resulting in altered hIgE function.

### Glycosylation in IgE biology and allergic disease

Here, we demonstrate that glycosylation of IgE is an absolute requirement for initiation of the allergic cascade. This requirement was mapped to a single, highly conserved N-linked site, occupied by oligomannose glycans. Selective removal of this glycan ablated interactions with FcεRI by altering conformation of IgE. The glycan is likely not involved in glycan–glycan or glycan–protein interactions with FcεRI, consistent with structural studies of IgE and FcεRI (Garman et al., 2000). This glycosylation site on IgE corresponds to the single site found on IgG Fcs, which governs IgG Fc–mediated effector functions (Garman et al., 2000). Our findings demonstrate a similar functional requirement for glycosylation of IgE, supporting a close evolutionary relationship shared by these Ig classes (Flajnik, 2002). Furthermore, *E. coli*–derived IgE required refolding in vitro to gain functionality, consistent with

mBMMCs determined by A647-OVA and mFcεRI ($n$ = 3; 2 independent experiments). (d) OVA-induced degranulation assayed by β-hexosaminidase in LAD2 cells sensitized with WT or αOVA-hIgE glycosylation mutants ($n$ = 3; 4 independent experiments). (e) OVA-induced PCA vascular leakage in hFcεRI$^{+}$/mFcεRI$^{-/-}$ mice by PBS, WT, or N394Q αOVA-hIgE ($n$ = 3; 2 independent experiments). (f) Binding of WT or αOVA-hIgE mutants to hFcεRI$^{+}$-HeLa cells as assessed by A647-OVA ($n$ = 2; 2 independent experiments). (g) Binding of increasing concentrations of WT or N394Q αOVA-hIgE to immobilized hFcεRIα in vitro (2 independent experiments.) Mean and SEM are plotted; ****, $P < 0.0001$; ***, $P < 0.001$; **, $P < 0.01$; ns, not significant.



Downloaded from jem.rupress.org on April 10, 2015

Published March 30, 2015



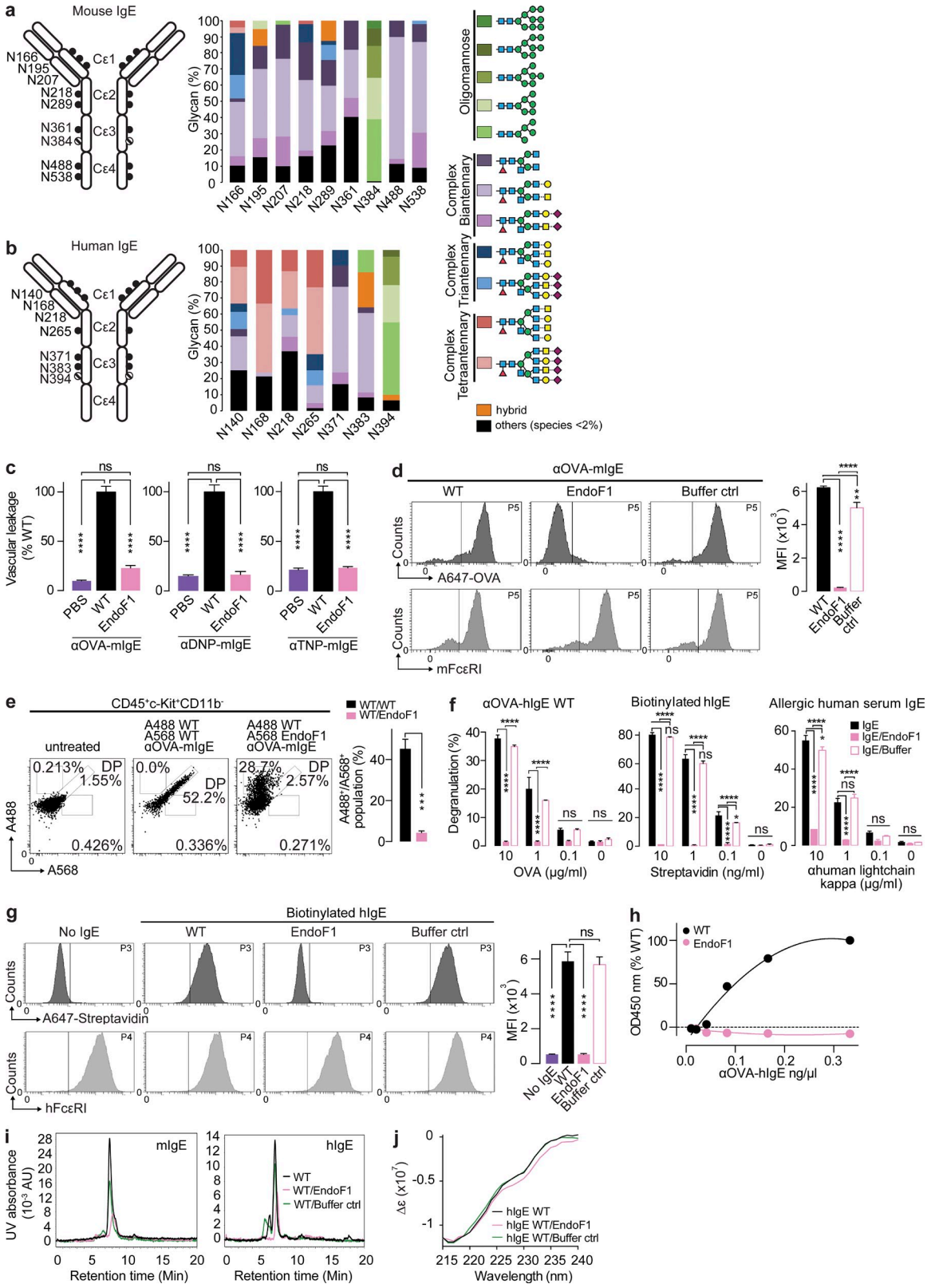


**Figure 4. Removal of the IgE oligomannose glycan abrogates anaphylaxis.** (a and b) αOVA-mIgE (a) and αOVA-hIgE (b) schematics with N-linked glycosylation consensus sites are shown. Percentages of glycan structures identified by glycopeptide mass spectroscopy at each site are plotted. Glycans are composed of fucose (red), N-acetylglucosamine (GlcNAc; blue), mannose (green), galactose (yellow circles), N-acetylgalactosamine (GalNAc; yellow squares), and sialic acid (pink); representative of two experiments. (c) PCA quantified after PBS, WT, or EndoF1-mIgE specific for OVA, DNP, or TNP ($n = 8$; 2 independent

Downloaded from jem.rupress.org on April 10, 2015

Published March 30, 2015



glycosylation playing a role in maintenance of the IgE Cε3 structure (Helm et al., 1988; Henry et al., 2000). Recently developed anti-IgE preventive therapies that neutralize circulating IgE or deplete IgE-producing cells have demonstrated some efficacy. However, clinical indications for these treatments have been limited to allergic asthma, chronic idiopathic urticarial, and rhinitis (Galli and Tsai, 2012; Gauvreau et al., 2014; Saini et al., 2015). Thus, the IgE oligomannose may be a potential therapeutic target for both cell-bound and circulating IgE. Furthermore, it is possible that variations in the glycan composition at the conserved site may explain why not all individuals with allergen-specific IgE suffer from allergies.

## MATERIALS AND METHODS

**Mice.** 5–6-wk-old BALB/c female mice were purchased from The Jackson Laboratory. hFcεRIα$^{+}$/mFcεRIα$^{-/-}$ and mFcεRIα$^{-/-}$ crossed at least 12 time to C57BL/6 mice (Dombrowicz et al., 1996) were maintained in the animal facility at Massachusetts General Hospital (MGH). Mice were all housed in specific pathogen–free conditions according to the National Institutes of Health (NIH), and all animal experiments were conducted under protocols approved by the Institutional Animal Care and Use Committee of MGH.

**Peanut extract preparation.** Unsalted dry-roasted peanuts (Blanched Jumbo Runner cultivar; Planters) were ground to a smooth paste, followed by washing with 20 vol cold acetone, filtered using Whatman paper, and dried. Protein was extracted by agitating the peanut flour overnight with PBS containing protease inhibitor cocktail without EDTA (Roche). The peanut protein extracts were collected as the supernatant after centrifugation at 24,000 *g* for 30 min.

**PCA.** Age- and sex-matched mice were randomized allocating to experimental group. 20 ng monoclonal mIgE specific for OVA, DNP (clone SPE-7; Sigma-Aldrich), or TNP (clone IgE-3; BD) or 5 ng polyclonal IgE specific for OVA or peanut extracts was injected intradermally in the BALB/c mice ears, and the next day mice were intravenously challenged with PBS containing 125 μg OVA (Sigma-Aldrich), peanut extract, DNP-HSA (Sigma-Aldrich), or TNP-BSA (conjugation ratio 13; Biosearch Technologies) and 2% Evans blue dye in PBS. 45 min after challenge, the mice were sacrificed and the ears were excised and minced before incubation in *N,N*-dimethylformamide (EMD Millipore) at 55°C for 3 h. The degree of blue dye in the ears was quantitated by the absorbance at 595 or 650 nm. For experiments of hIgE, 250 ng αOVA-hIgE was injected intradermally in hFcεRIα$^{+}$/mFcεRIα$^{-/-}$ or mFcεRIα$^{-/-}$ mice, followed by intravenous administration of OVA and Evans blue dye 4 h later.

**IgE antibodies.** To generate recombinant IgE antibodies, the variable and constant regions of heavy and light chains were individually cloned from OVA-specific Toε hybridoma (provided by H. Oettgen, Boston Children's Hospital, Harvard Medical School, Boston, MA), adapting from the protocol previously described (Morrison, 2002). Once the variable and the constant regions of heavy and light chain were joined by overlapping PCR, the heavy chain was placed under CMV promoter using restriction enzyme sites SalI and XbaI and the light chain was placed under EF1a promoter using restriction enzyme sites NotI and KpnI in pBUDCE4.1 expression vector (Invitrogen). A similar cloning strategy was used to construct αOVA-hIgE vector. The N-linked glycosylation sequons of IgE were mutated using the QuikChange II XL Site-Directed Mutagenesis kit (Agilent Technologies), according to the manufacturer's protocol. Recombinant antibodies were generated by transient transfection of the plasmids into HEK293T using Polyethylenimine "Max" (Polysciences, Inc.), followed by purification using *N*-hydroxysuccinimide–activated Sepharose beads (GE Healthcare) coupled to OVA (Sigma-Aldrich). Antibodies generated were verified by immunoblots for size and quantified by IgE ELISA, and the specificity was confirmed by OVA ELISA (see below).

Polyclonal IgE specific for OVA or peanut extracts was prepared by injecting BALB/c mice with 10 μg OVA (Sigma-Aldrich) or peanut extracts (preparation) in aluminum hydroxide on days 0, 7, and 14. Mice were bled on days 10, 17, 19, and 21. The sera was separated from the blood by serum gel tubes (BD) and depleted of IgG by incubating with Protein G high-capacity agarose beads (Thermo Fisher Scientific).

Human IgE was purified from de-identified peanut-allergic sera using *N*-hydroxysuccinimide–activated Sepharose beads coupled to omalizumab (Xolair; Genentech) after IgG depletion by Protein G high-capacity agarose beads. Purified IgE was verified by Coomassie and immunoblots and quantified by IgE ELISA. Patient sera were collected under protocols approved by the MGH Institutional Review Board.

**Fluorescent labeling and glycan digestion.** Human IgE (HE1 clone; Abcam) was biotinylated using the Biotin-XX Microscale Protein Labeling kit (Molecular Probes). WT- and N384Q-αOVA-mIgE were conjugated to Alexa Fluor 488 or Alexa Fluor 567 (Molecular Probes) according to the manufacturer's recommendations. IgE was digested with PNG (New England Biolabs, Inc.) or EndoF1 (Sigma-Aldrich) according to the manufacturer's instructions under nondenaturing conditions at 37°C for 72 h. All digestions were verified by lectin blot (see below).

**Immuno- and lectin blotting.** Immuno- and lectin blotting were performed as described previously (Anthony et al., 2008). In brief, equal amounts of protein were resolved on 3–8% Tris-Acetate protein gels (Life Technologies) in SDS-PAGE under nonreducing conditions. After transfer to polyvinylidene difluoride membranes, membranes were blocked with 5% dry milk in PBS containing 0.05% Tween 20 for immunoblotting or with Protein-Free Blocking Buffers (Thermo Fisher Scientific) for lectin blotting. Mouse or human IgE was probed by goat polyclonal anti–mouse or anti–human IgE-HRP (10 ng/ml; Bethyl Laboratories, Inc.), respectively. N-linked glycans were detected by biotinylated *Lens culinaris* agglutinin (LCA; 5 μg/ml; Vector Laboratories) and α1,3- and α1,6-linked high mannose structures were detected by biotinylated *Galanthus nivalis* lectin (GNA; 4 μg/ml; Vector Laboratories).

**ELISA.** Mouse or human IgE was quantified by sandwich ELISA according to instructions from mouse or human IgE ELISA quantitation sets (Bethyl Laboratories, Inc.). Antibodies specific for OVA were verified by 96-well Nunc plates plate coated with 75 μg/ml OVA (Sigma-Aldrich), blocked with 2% BSA in PBS, and probed with goat polyclonal anti–mouse or anti–human IgE-HRP (2 ng/ml; Bethyl Laboratories, Inc.). A similar protocol

experiments). (d) Histograms and MFI of WT-, EndoF1-, and EndoF1 buffer only–αOVA-mIgE bound to mBMMCs determined by A647-OVA and mFcεRI FACS ($n$ = 3; 2 independent experiments). (e) Scatter plots of dermal mast cells recovered from ears injected with A488-WT- and A568-WT- or A488-WT- and A568-EndoF1-αOVA-mIgE ($n$ = 2; 2 independent experiments). (f) β-Hexosaminidase activity after stimulation by OVA, streptavidin, or anti–human kappa light chain in LAD2 cells sensitized with αOVA-hIgE, biotinylated hIgE, or allergic human serum IgE or hIgE treated with EndoF1 or EndoF1 buffer only ($n$ = 3; 2 independent experiments). (g) Binding of WT, EndoF1, or EndoF1 buffer only biotinylated hIgE to hFcεRI-HeLa cells as assessed by FACS ($n$ = 3; 2 independent experiments). (h) Quantitation of WT or EndoF1-treated αOVA-hIgE bound to immobilized hFcεRIα (2 independent experiments). (i) Size exclusion chromatography profile of αOVA-mIgE or hIgE treated with EndoF1 or buffer only. (j) CD spectra of WT, EndoF1-treated, or EndoF1 buffer control hIgE (representative of two experiments). Mean and SEM are plotted; ****, $P < 0.0001$; ***, $P < 0.001$; **, $P < 0.01$; *, $P < 0.05$; ns, not significant.



Downloaded from jem.rupress.org on April 10, 2015

Published March 30, 2015



was used for verifying antibodies specific for DNP and TNP, except 5 μg/ml DNP-HSA (Sigma-Aldrich) and TNP-BSA (conjugation ratio 13; Biosearch Technologies) was used for coating. All reactions were detected by 3,3,5,5-tetramethylbenzidine (TMB; Thermo Fisher Scientific) and stopped by 2 M sulfuric acid, and the absorbance was measured at 450 nm.

**LAD2 mast cell culture.** Human LAD2 mast cell line (from D. Metcalfe, National Institute of Allergy and Infectious Diseases, NIH, Bethesda, MD) was cultured in StemPro-34 SFM medium (Life Technologies) supplemented with 2 mM L-glutamine, 100 U/ml penicillin, 100 μg/ml streptomycin, and 100 ng/ml recombinant human stem cell factor (PeproTech). The cells were hemi-depleted each week with fresh medium and maintained at 0.25–5 × $10^5$ cells/ml at 37°C and 5% $CO_2$.

**Human mast cell degranulation assay.** Degranulation was measured as described previously (Kuehn et al., 2010). In brief, LAD2 cells were sensitized with 250 ng αOVA-hIgE, 100 ng biotinylated hIgE, or 25 ng allergic human serum IgE overnight. Upon OVA or streptavidin (Sigma-Aldrich) activation, the level of mast cell degranulation was monitored by the release of β-hexosaminidase in mast cell granules, quantified by the extent of its substrate *p*-nitrophenyl *N*-acetyl-β-D-glucosamide (PNAG) digested in a colorimetric assay.

**IgE-FcεRI binding assay and flow cytometry.** mBMMCs were generated by flushing BM precursors from tibias and femurs of C57BL/6 mice and culturing in RPMI supplemented with 10% fetal bovine serum, 2 mM L-glutamine, 100 U/ml penicillin, 100 μg/ml streptomycin, 10 ng/ml recombinant mouse IL-3 (BioLegend), and 10 ng/ml mouse stem cell factor (PeproTech) for 4–6 wk at 37°C in 5% $CO_2$. HeLa cells that express human FcεRI- α, -β, and -γ chains (hFcεRI$^+$-HeLa cells) were generated by retroviral transduction. BMMCs or hFcεRI$^+$-HeLa cells were incubated overnight with 100 ng of mouse or human IgE, respectively. Cells were washed to remove unbound IgE before incubation with A647-OVA (500 ng/ml; Molecular Probes) for OVA-specific IgE or Alexa Fluor 647–streptavidin (1:200 dilution; BioLegend) for biotinylated hIgE for 10 min at 37°C. FcεRI expression of the IgE-sensitized cells was confirmed by staining with PE-labeled anti-hFcεRIα (CRA1-PE clone AER-37; eBioscience) and anti-mFcεRIα (MAR1-PE; BioLegend). Flow cytometric analysis was performed using the FACSCanto II and FACSDiva software (BD).

**Saturation binding assays.** The extracellular portion of the α chain of hFcεRI (shFcεRIα) was cloned from cDNA of human myeloid dendritic cells into HindIII and BamHI sites of p3x-FLAG-CMV-13 (Sigma-Aldrich) to generate shFcεRIα-flag. The plasmid was transiently transfected into HEK293T cells as described above, and shFcεRIα-flag protein was purified from culture supernatants using anti-flag M2 affinity gel (Sigma-Aldrich) per the manufacturer's instructions. 96-well Nunc plates were coated with shFcεRIα-flag (10 ng/μl), blocked with 2% BSA in PBS, and incubated with increasing concentrations of WT- and N394Q-αOVA-hIgE or hIgE (Abcam) and EndoF1-treated hIgE. After 30 min, the wells were washed, and shFcεRIα-flag–bound hIgE was probed by anti–Fab-HRP (Bethyl Laboratories, Inc.) and detected by TMB. The reactions were stopped by 2 M sulfuric acid, and the absorbance measured at 450 nm.

**Size-exclusion chromatography.** IgE monomers and aggregates were resolved in 150 mM sodium phosphate, pH 7.0, containing 1.5 μM Bis-ANS (4,4′-Dianilino-1,1′-Binaphthyl-5,5′-Disulfonic Acid, Dipotassium Salt) using an HPLC outfitted with a Sepax Zenix-C HP-SEC column 4.6 × 300 mm, 3 μm particle size, and detected by UV at 280 nm. The column was maintained at 30°C and the flow rate at 350 μl/min.

**Glycopeptide mass spectrometry analysis and data analysis.** Site-specific glycosylation was quantified for both the recombinant αOVA-mIgE and αOVA-hIgE using nano LC-MS/MS after enzymatic digestion of the proteins, as previously described (Plomp et al., 2014). Most sites were quantified from the tryptic digest based on the extracted ion current for the most abundant charge state for each of the peptides, except chymotrypsin was used for the analysis of N140 and N168 from αOVA-hIgE and N166, N195, and N207 from αOVA-mIgE. The isolated IgE was prepared for proteolysis by denaturing the protein in 6M guanidine HCl, followed by reduction with dithiothreitol and alkylation with iodoacetamide. The enzymatic digests were performed in 25 mM ammonium bicarbonate, pH 7.8, overnight (trypsin) or for 4 h (chymotrypsin). The digestion was quenched with formic acid added to 2% wt/wt. The separation was performed on an EasySpray C18 nLC column 0.75 μm × 50 cm (Thermo Fisher Scientific) using water and acetonitrile with 0.1% formic acid for mobile phase A and mobile phase B, respectively. A linear gradient from 1 to 35% mobile phase B was run 120 min. Mass spectra were recorded on a QExactive mass spectrometer (Thermo Fisher Scientific) operated in positive mode and using a top 12 data–dependent method. Glycopeptides were quantified in QualBrowser (Thermo Fisher Scientific) based on the extracted ion area for the most abundant charge state for each glycopeptide. The relative abundance was calculated for all identified glycan species for each site using Excel (Microsoft).

Glycopeptides were quantified based on the extracted ion area for abundant charge state for each glycopeptide. The relative abundance was calculated for all identified glycan species for each site without the use of internal standards making the relative abundances subject to the influence of ionization efficiency. The extracted ion chromatograms for the major and minor species from N394 are shown in Fig. S2 a. Identification of the glycopeptides was based on the presence of the oxonium ions 366.14 (Hex-HexNAc) and 204.08 (HexNAc) common to all glycosylated peptides, as well as the Y1 ion (peptide + HexNAc) which is unique to each site.

In cases where multiple chromatographic peaks were seen for a single mass, higher-energy collisionally activated dissociation (HCD) MS/MS was used for identifying differences between the chromatographically resolved isomers. Fig. S2 c shows the comparison of three neutral glycopeptides having the same apparent molecular weight. The $MS^2$ spectrum for the first chromatographic peak shows evidence of a HexNAc-HexNAc structure with a mass of 407.16 D, supporting the assignment of this species as containing terminal *N*-acetylgalactosamine. The second peak shows evidence of a HexNAc-Hex-HexNAc structure at 569.20 not seen in the $MS^2$ from the first chromatographic peak. Unique Y ions at 1804.81 and 1950.87 in this second spectrum support the assignment of isomer 2 as containing bisecting *N*-acetylglucosamine.

The $MS^2$ was also used to differentiate between species of similar mass with different composition. The $MS^2$ comparison in Fig. S2 d shows the fragmentation pattern for a trifucosylated glycopeptide (top panel) from hIgE N371 with three sialylated/core-fucosylated glycopeptide (bottom three panels) from the same site. In Fig. S2 d, both oxonium (B) ions and Y ions were useful for elucidating the structure. The comparison of the $MS^2$ spectra in the second and third panel from the top in Fig. S2 d suggests the major difference between these species is the location of the sialic acid. The oxonium ion at 495.17 from the $MS^2$ spectrum in panel 2 of Fig. S2 d suggests a GalNAc-NeuAc linkage, whereas Gal-NeuAc is more likely the structure in the third panel based on the ion at 657.23. These spectra are representative of the data used to assign likely structures for each of the sites on both mIgE and hIgE.

**CD.** Untreated human IgE (HE1 clone; Abcam) or human IgE digested with EndoF1 or EndoF1 buffer was exchanged into 10 mM sodium phosphate buffer, pH 7.0, and concentrated to 0.1 μg/μl. The CD spectra of IgE were acquired in a J-815 spectropolarimeter (Jasco) in a 1-mm quartz cell. Data were acquired in the far UV range (245–195 nm), and a total of four scans were averaged for each sample. Cells were maintained at 23°C using a bandwidth of 1 nm and a 4-s response time. Ellipticity is expressed in molar CD ($\Delta\varepsilon$), where $\Delta\varepsilon = \theta(\text{Obs}) \times$ mean residue weight/10× solute concentration (C) × path length (l) × 3,298.

**Flow cytometry.** Untreated ears or ears that were intradermally injected with fluorescently labeled αOVA-mIgE 16 h prior were separated into dorsal and ventral halves and minced before digestion with Liberase (Roche) and subjected to disruption, to generate single cell suspensions, as previously

Downloaded from jem.rupress.org on April 10, 2015

described (Riol-Blanco et al., 2014). Suspension cells were resuspended in PBS and incubated with Zombie Yellow Fixable Viability kit (BioLegend) before incubation with anti–mouse CD16/CD32 (clone 93) in FACS buffer (2 mM EDTA and 0.5% BSA in PBS). Antibodies for surface antigen staining included Alexa Fluor 647 anti–mouse CD117 (c-Kit; clone 2B8; BioLegend), Pacific Blue anti–mouse CD45 (clone 30-F11; BioLegend), PE/Cy7 anti–mouse/human CD11b (clone M1/70; BioLegend), FITC anti–mouse CD8 (clone 53-6.7; BioLegend), PE anti–mouse CD8 (clone 53-6.7; BioLegend), APC anti–mouse CD8 (clone 53-6.7; BioLegend), and PE/Cy7 anti–mouse CD8 (clone 53-6.7; BioLegend). Cells were resuspended in FACS buffer after staining and acquired using an LSRII flow cytometer (BD). Data were analyzed using FlowJo version 7.6 software (Tree Star).

**Statistical analyses.** All statistical analyses were performed using Prism 6 (GraphPad Software), and results are shown as means with SEM. An unpaired Student's *t* test was used to compare two unmatched groups. For the comparison between three or more groups, one-way or two-way ANOVA with Bonferroni's multiple comparisons test was used. Statistical power was not used to determine sample size.

**Online supplemental material.** Fig. S1 shows the gating strategy for identifying dermal mast cells. Fig. S2 shows glycopeptide mass spectrometry of recombinant mouse and human IgE. Tables S1 and S2, included as separate Excel files, show primary glycopeptide mass spectrometry data from mIgE and hIgE, respectively. Online supplemental material is available at http://www.jem.org/cgi/content/full/jem.20142182/DC1.

We are grateful to Andrew D. Luster, Fredrik Wermeling, and Kate L. Jeffrey for careful reading of the manuscript, Wayne Shreffler for providing de-identified patient samples, Bert Ruiter for providing peanut extract preparations, and Maya Kitaoka for excellent technical support.

This work was supported by National Institutes of Health grants U19AI095261 and 1K22AI091684 to R.M. Anthony, R01CA150975 to T.R. Mempel, K01DK093597 to B. Platzer, and RO1AI075037 to E. Fiebiger; Harvard Digestive Diseases Center grant P30DK034854 to E. Fiebiger; and a Mizutani Foundation for Glycoscience Research Grant to R.M. Anthony.

The authors declare no competing financial interests.

**Submitted: 21 November 2014**
**Accepted: 11 March 2015**

## REFERENCES

Anthony, R.M., F. Nimmerjahn, D.J. Ashline, V.N. Reinhold, J.C. Paulson, and J.V. Ravetch. 2008. Recapitulation of IVIG anti-inflammatory activity with a recombinant IgG Fc. *Science*. 320:373–376. http://dx.doi.org/10.1126/science.1154315

Arnold, J.N., M.R. Wormald, R.B. Sim, P.M. Rudd, and R.A. Dwek. 2007. The impact of glycosylation on the biological function and structure of human immunoglobulins. *Annu. Rev. Immunol.* 25:21–50. http://dx.doi.org/10.1146/annurev.immunol.25.022106.141702

Basu, M., J. Hakimi, E. Dharm, J.A.J. Kondas, W.H.W. Tsien, R.S.R. Pilson, P. Lin, A. Gilfillan, P. Haring, E.H.E. Braswell, et al. 1993. Purification and characterization of human recombinant IgE-Fc fragments that bind to the human high affinity IgE receptor. *J. Biol. Chem.* 268:13118–13127.

Björklund, J.E.M., T. Karlsson, and C.G.M. Magnusson. 1999. N-glycosylation influences epitope expression and receptor binding structures in human IgE. *Mol. Immunol.* 36:213–221. http://dx.doi.org/10.1016/S0161-5890(99)00036-X

Björklund, J.E.M., M. Schmidt, and C.G.M. Magnusson. 2000. Characterisation of recombinant human IgE-Fc fragments expressed in baculovirus-infected insect cells. *Mol. Immunol.* 37:169–177. http://dx.doi.org/10.1016/S0161-5890(00)00028-6

Dombrowicz, D., V. Flamand, K.K. Brigman, B.H. Koller, and J.-P. Kinet. 1993. Abolition of anaphylaxis by targeted disruption of the high affinity immunoglobulin E receptor α chain gene. *Cell*. 75:969–976. http://dx.doi.org/10.1016/0092-8674(93)90540-7

Dombrowicz, D., A.T. Brini, V. Flamand, E. Hicks, J.N. Snouwaert, J.P. Kinet, and B.H. Koller. 1996. Anaphylaxis mediated through a humanized high affinity IgE receptor. *J. Immunol.* 157:1645–1651.

Dorrington, K.J., and H.H. Bennich. 1978. Structure-function relationships in human immunoglobulin E. *Immunol. Rev.* 41:3–25. http://dx.doi.org/10.1111/j.1600-065X.1978.tb01458.x

Feige, M.J., S. Nath, S.R. Catharino, D. Weinfurtner, S. Steinbacher, and J. Buchner. 2009. Structure of the murine unglycosylated IgG1 Fc fragment. *J. Mol. Biol.* 391:599–608. http://dx.doi.org/10.1016/j.jmb.2009.06.048

Flajnik, M.F. 2002. Comparative analyses of immunoglobulin genes: surprises and portents. *Nat. Rev. Immunol.* 2:688–698. http://dx.doi.org/10.1038/nri889

Galli, S.J., and M. Tsai. 2012. IgE and mast cells in allergic disease. *Nat. Med.* 18:693–704. http://dx.doi.org/10.1038/nm.2755

Garman, S.C., B.A. Wurzburg, S.S. Tarchevskaya, J.P. Kinet, and T.S. Jardetzky. 2000. Structure of the Fc fragment of human IgE bound to its high-affinity receptor FcεRIα. *Nature*. 406:259–266. http://dx.doi.org/10.1038/35018500

Gauvreau, G.M., J.M. Harris, L.-P. Boulet, H. Scheerens, J.M. Fitzgerald, W.S. Putnam, D.W. Cockcroft, B.E. Davis, R. Leigh, Y. Zheng, et al. 2014. Targeting membrane-expressed IgE B cell receptor with an antibody to the M1 prime epitope reduces IgE production. *Sci. Transl. Med.* 6:243ra85. http://dx.doi.org/10.1126/scitranslmed.3008961

Gould, H.J., B.J. Sutton, A.J. Beavil, R.L. Beavil, N. McCloskey, H.A. Coker, D. Fear, and L. Smurthwaite. 2003. The biology of IGE and the basis of allergic disease. *Annu. Rev. Immunol.* 21:579–628. http://dx.doi.org/10.1146/annurev.immunol.21.120601.141103

Helm, B., P. Marsh, D. Vercelli, E. Padlan, H. Gould, and R. Geha. 1988. The mast cell binding site on human immunoglobulin E. *Nature*. 331:180–183. http://dx.doi.org/10.1038/331180a0

Henry, A.J.A., J.M.J. McDonnell, R. Ghirlando, B.J.B. Sutton, and H.J.H. Gould. 2000. Conformation of the isolated Cε3 domain of IgE and its complex with the high-affinity receptor, FcεRI. *Biochemistry*. 39:7406–7413. http://dx.doi.org/10.1021/bi9928391

Hunt, J., R.L. Beavil, R.A. Calvert, H.J. Gould, B.J. Sutton, and A.J. Beavil. 2005. Disulfide linkage controls the affinity and stoichiometry of IgE Fcε3–4 binding to FcεRI. *J. Biol. Chem.* 280:16808–16814. http://dx.doi.org/10.1074/jbc.M500965200

Kuehn, H.S., M. Radinger, and A.M. Gilfillan. 2010. Measuring mast cell mediator release. *Curr. Protoc. Immunol.* Chapter 7:38.

Marichal, T., P. Starkl, L.L. Reber, J. Kalesnikoff, H.C. Oettgen, M. Tsai, M. Metz, and S.J. Galli. 2013. A beneficial role for immunoglobulin E in host defense against honeybee venom. *Immunity*. 39:963–975. http://dx.doi.org/10.1016/j.immuni.2013.10.005

Matsumoto, M., Y. Sasaki, K. Yasuda, T. Takai, M. Muramatsu, T. Yoshimoto, and K. Nakanishi. 2013. IgG and IgE collaboratively accelerate expulsion of *Strongyloides venezuelensis* in a primary infection. *Infect. Immun.* 81:2518–2527. http://dx.doi.org/10.1128/IAI.00285-13

Morrison, S.L. 2002. Cloning, expression, and modification of antibody V regions. *Curr. Protoc. Immunol.* Chapter 2:12.

Nettleton, M.Y., and J.P. Kochan. 1995. Role of glycosylation sites in the IgE Fc molecule. *Int. Arch. Allergy Immunol.* 107:328–329. http://dx.doi.org/10.1159/000237017

Palm, N.W., R.K. Rosenstein, S. Yu, D.D. Schenten, E. Florsheim, and R. Medzhitov. 2013. Bee venom phospholipase A2 induces a primary type 2 response that is dependent on the receptor ST2 and confers protective immunity. *Immunity*. 39:976–985. http://dx.doi.org/10.1016/j.immuni.2013.10.006

Pawankar, R., S.T. Holgate, G.W. Canonica, R.F. Lockey, and M.S. Blaiss. 2013. World Allergy Organization (WAO) White Book on Allergy: Update 2013. World Allergy Organization, Milwaukee, WI. 248 pp.

Plomp, R., P.J. Hensbergen, Y. Rombouts, G. Zauner, I. Dragan, C.A.M. Koeleman, A.M. Deelder, and M. Wuhrer. 2014. Site-specific N-glycosylation analysis of human immunoglobulin E. *J. Proteome Res.* 13:536–546. http://dx.doi.org/10.1021/pr400714w

Riol-Blanco, L., J. Ordovas-Montanes, M. Perro, E. Naval, A. Thiriot, D. Alvarez, S. Paust, J.N. Wood, and U.H. von Andrian. 2014. Nociceptive

Downloaded from jem.rupress.org on April 10, 2015

Published March 30, 2015



sensory neurons drive interleukin-23-mediated psoriasiform skin inflammation. *Nature*. 510:157–161. http://dx.doi.org/10.1038/nature13199

Saini, S.S., C. Bindslev-Jensen, M. Maurer, J.-J. Grob, E. Bülbül Baskan, M.S. Bradley, J. Canvin, A. Rahmaoui, P. Georgiou, O. Alpan, et al. 2015. Efficacy and safety of omalizumab in patients with chronic idiopathic/spontaneous urticaria who remain symptomatic on H1 antihistamines: a randomized, placebo-controlled study. *J. Invest. Dermatol.* 135:67–75. http://dx.doi.org/10.1038/jid.2014.306

Sayers, I., S.A. Cain, J.R. Swan, M.A. Pickett, P.J. Watt, S.T. Holgate, E.A. Padlan, P. Schuck, and B.A. Helm. 1998. Amino acid residues that influence FcεRI-mediated effector functions of human immunoglobulin E. *Biochemistry*. 37:16152–16164. http://dx.doi.org/10.1021/bi981456k

Sondermann, P., A. Pincetic, J. Maamary, K. Lammens, and J.V. Ravetch. 2013. General mechanism for modulating immunoglobulin effector function. *Proc. Natl. Acad. Sci. USA*. 110:9868–9872. http://dx.doi.org/10.1073/pnas.1307864110

Young, R.J.R., R.J.R. Owens, G.A.G. Mackay, C.M.C. Chan, J. Shi, M. Hide, D.M.D. Francis, A.J.A. Henry, B.J.B. Sutton, and H.J.H. Gould. 1995. Secretion of recombinant human IgE-Fc by mammalian cells and biological activity of glycosylation site mutants. *Protein Eng.* 8:193–199. http://dx.doi.org/10.1093/protein/8.2.193

Downloaded from jem.rupress.org on April 10, 2015

The Journal of Experimental Medicine

## SUPPLEMENTAL MATERIAL

**Shade et al., http://www.jem.org/cgi/content/full/jem.20142182/DC1**

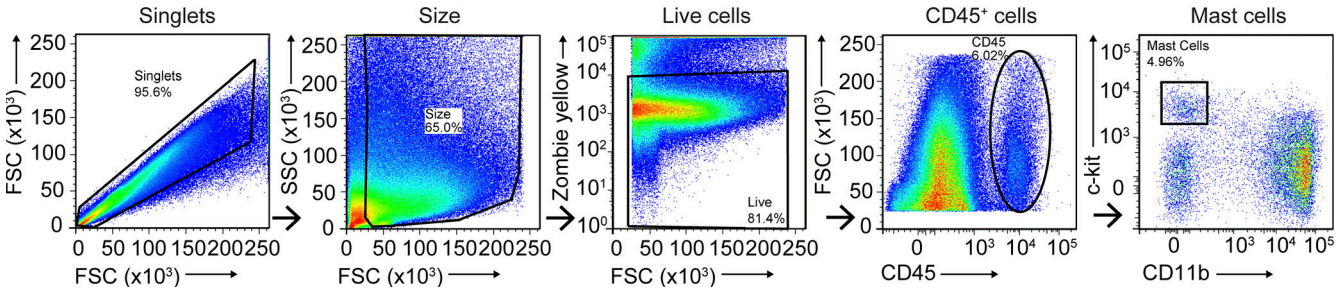


**Figure S1. Gating strategy for identifying dermal mast cells.** Single cell suspensions of ear dermal cells were analyzed by flow cytometry. Representative singlet, forward and side scatter (FSC and SSC), live cell, leukocyte (CD45⁺), and mast cell (c-Kit⁺ CD11b⁻) gates are shown.

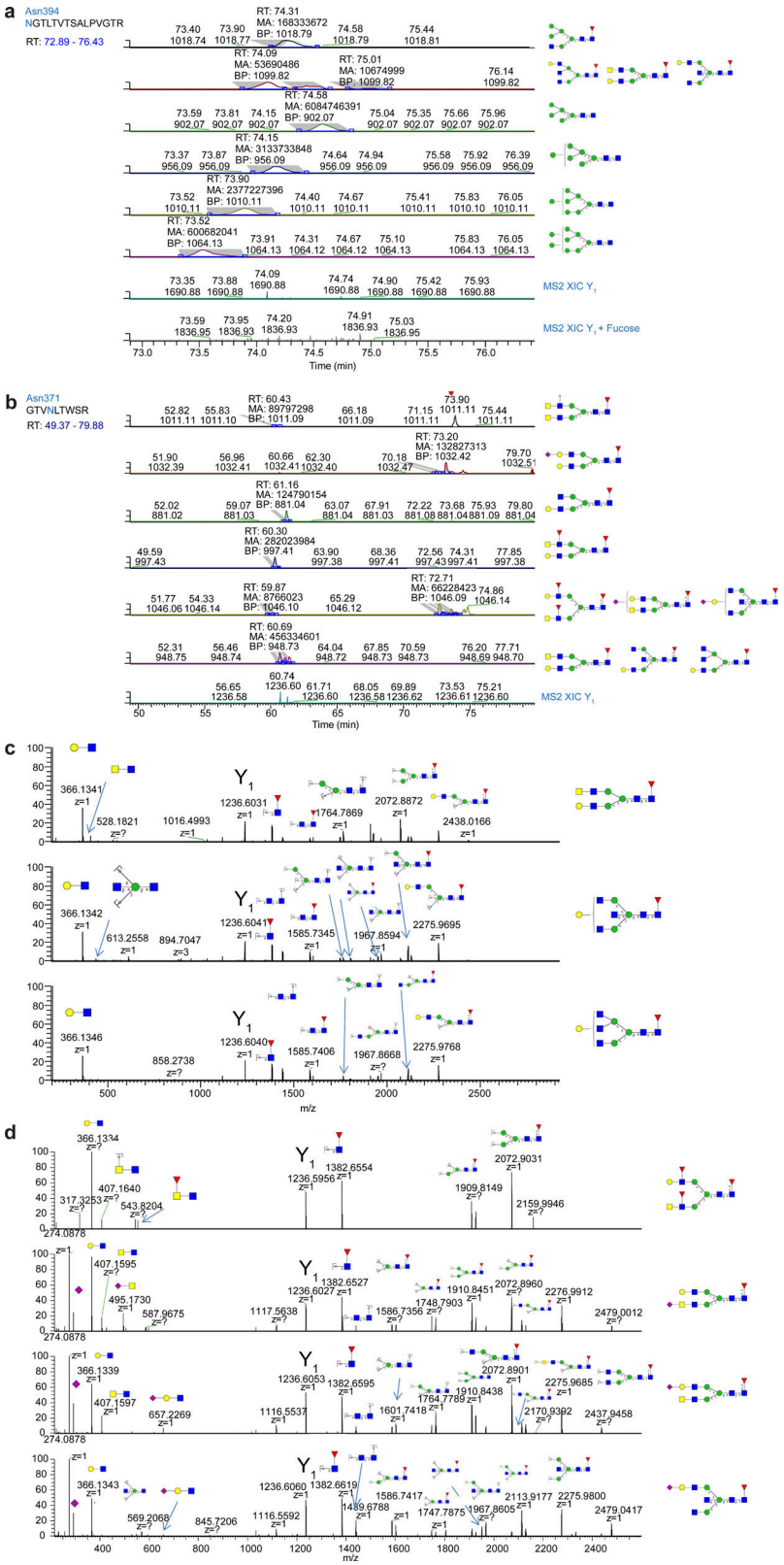


**Figure S2. Glycopeptide mass spectrometry of recombinant mouse and human IgE.** (a) Primary data used to generate percentages shown in Fig. 4 (a and b) are given. (b) Representative histograms of LC-MS runs, plotted as LC over mass to charge ratio (m/z) are shown. (c) Representative histograms from HCD MS/MS used for identifying differences where multiple chromatographic peaks were seen for a single mass show the comparison of three neutral glycopeptides having the same apparent molecular weight. (d) Representative histograms of MS/MS comparing the fragmentation pattern for a trifucosylated glycopeptide (top) from hIgE N371 with three sialylated/core-fucosylated glycopeptide (bottom three panels) from the same site.

**Tables S1 and S2, included as separate Excel files, show primary glycopeptide mass spectrometry data from mIgE and hIgE, respectively.**